Collisionally Activated Dissociation and Electron Capture Dissociation Provide Complementary Structural Information for Branched Permethylated Oligosaccharides

Cheng Zhao,[a,b]* Bo Xie,[a]* Shiu-Yung Chan,[a] Catherine E. Costello,[a,b] and Peter B. O'Connor[a,b]

[a] Mass Spectrometry Resource, Department of Biochemistry, Boston University School of Medicine, Boston, Massachusetts, USA
[b] Cardiovascular Proteomics Center, Boston University School of Medicine, Boston, Massachusetts, USA

Doubly charged sodiated and permethylated linear malto-oligosaccharides ($\{Glc\}_6$-$\{Glc\}_9$), branched *N*-linked glycans (high-mannose type $GlcNAc_2Man_{5\text{-}9}$, and complex asialo- and disialylated-biantennary glycans) were analyzed by tandem mass spectrometry using collisionally-activated dissociation (CAD) and "hot" electron capture dissociation (ECD) available in a custom-built ESI FTICR mass spectrometer. For linear permethylated malto-oligosaccharides, both CAD and "hot" ECD produced glycosidic cleavages (B, Y, C, and Z ions), cross-ring cleavages (A- and X-type), and internal cleavages (B/Y and C/Y type) to provide sequence and linkage information. For the branched *N*-linked glycans, CAD and "hot" ECD provided complementary structural information. CAD generated abundant B and Y fragment ions by glycosidic cleavages, whereas "hot" ECD produced dominant C and Z ions. A-type cross-ring cleavages were present in CAD spectra. Complementary A- and X-type cross-ring fragmentation pairs were generated by "hot" ECD, and these delineated the branching patterns and linkage positions. For example, $^{0,4}A_n$ and $^{3,5}A_n$ ions defined the linkage position of the major branch as the 6-position of the central core mannose residue. The internal fragments observed in CAD were more numerous and abundant than in "hot" ECD spectra. Since the triply charged (sodiated) molecular ion of the permethylated disialylated-biantennary *N*-linked glycan has relatively high abundance, it was isolated and fragmented in a "hot" ECD experiment and extensive fragment ions (glycosidic and complementary pairs of cross-ring cleavages) were generated to fully confirm the sequence, branching, and linkage assignments for this glycan. (J Am Soc Mass Spectrom 2008, 19, 138–150) © 2008 American Society for Mass Spectrometry

Biological carbohydrates constitute diverse types of biopolymers playing various roles in cellular processes, such as energy storage (glycogen), structural support (cellulose, chitin), signaling, protein folding, targeting and turnover, and extracellular interactions [1, 2]. Membrane associated carbohydrates are generally in the form of oligosaccharides covalently attached to proteins (glycoproteins) and or lipid (glycolipids). *O*-glycosylation, which involves covalent attachment of an oligosaccharide through an ether linkage to a lipid or to a protein through the side-chain oxygen in serine or threonine and *N*-glycosylation through the side-chain amide nitrogen in asparagine, are two key types of glycosylation. In cases of *N*-glycosylation, a common pentasaccharide core [3] is attached to asparagine in the consensus sequence Asn-X-Ser/Thr, where X may be any amino acid except proline. "High-mannose", "complex", and "hybrid" glycans, the three main classes of *N*-glycosylation, are distinguished from one another on the basis of the saccharide units that extend beyond the common core.

Unlike linear biomolecules such as DNA, RNA, and proteins, carbohydrates can form complicated, highly branched structures whose saccharide units are connected to each other through a variety of linkage types. Since even minor differences in linkage or branching may have profound effects on the 3D conformation and the biological activity, structural characterization of carbohydrates requires determination of not only glycan residue sequence information, but also linkage and branching information [4, 5]. Although exoglycosidases are frequently used for sequence analysis, mass spectral fragmentation is becoming more generally accepted as there can be problems in obtaining exoglycosidases that have sufficient purity and specificity, and mass spec-

Address reprint requests to Professor Peter B. O'Connor, Mass Spectrometry Resource, Boston University School of Medicine, 670 Albany Street, Room 507, Boston, MA 02118-2646, USA. E-mail: poconnor@bu.edu

* These two authors contributed equally to this work.

1044-0305/08/$32.00
doi:10.1016/j.jasms.2007.10.022

Published online November 7, 2007
Received April 27, 2007
Revised October 25, 2007
Accepted October 25, 2007

trometers are now available that can produce high quality glycan and glycoconjugate MS/MS spectra [6–10] from small amounts of material. Electrospray (ESI) [11] and matrix-assisted laser desorption (MALDI) [12, 13] are now the most popular ionization sources used in carbohydrate structural analysis [14–17]. Fourier-transform (FT) mass spectrometers using either ESI or MALDI ionization sources, provide powerful instrumentation for structural analysis of carbohydrates due to their superior resolving power and mass accuracy [18, 19]. Furthermore, Fourier-transform mass spectrometers are highly flexible because MS/MS experiments can utilize a variety of fragmentation techniques that are applied both external to the ICR cell (such as nozzle–skimmer collision ally activated dissociation (CAD) [20], or Q2 CAD [6, 7, 21, 22], and within the ICR cell (e.g., sustained off-resonance irradiation collision-activated dissociation (SORI-CAD) [23, 24], infrared multiphoton dissociation (IRMPD) [25], electron–capture dissociation (ECD) [26–29], and electron detachment dissociation (EDD) [30–32].

The combination of ECD with CAD or IRMPD in FTMS [33–36] can provide extensive and complementary information about biomolecule primary structure. For *N*-glycosylated peptides, IRMPD [19, 25, 33, 37–39] causes extensive cleavage of the glycosidic bonds while CAD [40–42] also cleaves the peptide backbone and ECD [26, 33, 37, 39, 43–46] cleaves the peptide backbone without extensive dissociation within the glycans. Thus, current literature suggests that IRMPD provides more specific glycan sequence information.

In addition, the structural analysis of glycans can also be achieved by fragmenting the glycans released by chemical (e.g., hydrazine [47–49], NaOH, NH_4OH), or glycosidase [49, 50] treatment of the glycoprotein or proteolytically generated glycopeptides. MS/MS experiments on glycans generate fragments resulting from glycosidic cleavages between the sugar rings and cross-ring cleavages within the rings. Internal cleavages are also generated from multiple glycosidic cleavages. The glycosidic, internal, and cross-ring fragment ions can provide sequence information, and cross-ring fragment ions can also provide branching and linkage information. Cross-ring fragment ions are mainly produced by pericyclic retro-aldol and retro-ene mechanisms [51]. The nomenclature generally used for describing glycan fragment ions is that introduced by Domon and Costello [52] in 1988 (Supplemental Figure S1, which can be found in the electronic version of this article); ions retaining a charge on the nonreducing terminus are named A (cross-ring), B, and C (glycosidic) whereas those ions retaining a charge on the reducing terminus are X (cross-ring), Y, and Z (glycosidic).

The product ion patterns of native glycan $[M + H]^+$ ions fragmented by CAD are relatively simple and not particularly informative as CAD produces mainly B-, Y- and B/Y internal cleavage ions. Cross-ring cleavage ions are generally absent. An important complicating factor is the appearance of rearrangement ions, particularly from native glycans or glycans derivatized at the reducing terminus [53–57]. High-energy CAD of native glycans [51, 58, 59] cause some cross-ring cleavages but most modern instruments cannot perform this experiment. Fragmentation of $[M + Li]^+$ and $[M + Na]^+$ ions from *N*-linked glycans produced a higher percentage of cross-ring cleavage reactions than fragmentation of $[M + H]^+$ ions, [60–62], and Lebrilla [63–67] and Leary [68–72] have extensively studied the fragmentation patterns of metal adducted oligosaccharides under CAD and IRMPD conditions with the general trend that larger metals stabilize oligosaccharides—particularly those containing sialic acid. In general, A-type cross-ring fragments are present in CAD and IRMPD, though they generally have fairly low abundances in the low-energy spectra. The $^{0,4}A_n$ and $^{3,5}A_n$ ions from cleavage within the central core mannose are usually present and can be used to define the compositions of the individual antennae attached to the core mannose. However, the presence of many internal fragments produced by multiple pathways complicates spectral interpretation. Budnik et al. [73] have compared ECD, EID (also known as EIEIO [74]), and CAD on the sodiated penta β1,4-linked *N*-acetylglucosamide $(GlcNAc)_5$ and concluded that EID was more effective than CAD but CAD resulted in the complete series of $^{0,2}A_n$ and $^{2,4}A_n$ cross-ring ion products. Upon further study of the spectra reported, it seems highly likely that the results Budnik et al. [73] reported were actually a combination of EID (vibrational excitation by collision with an electron—without electron capture) and "hot" ECD because the fragments observed included odd-electron fragments commonly observed with ECD. Studies including negative CAD [75–77] and EDD [30–32] have shown that negative ion tandem mass spectrometry of native glycans and glycosaminoglycans provide more cross-ring cleavages than positive ion mode.

As is well known, permethylation decreases the extent of intermolecular hydrogen bonding and eliminates facile dehydration, thus making glycans more volatile and less susceptible to decomposition during transfer to the gas phase. It also increases the hydrophobicity of glycans, so that the permethylated glycans migrate to the surface of the electrospray droplets. Surface molecules on the droplet have increased probabilities to retain the charge when the droplet evaporates, thus further increasing sensitivity [10, 17, 78, 79].

In this study, both CAD and "hot" ECD experiments were performed on a series of sodiated and permethylated glycans, to study their fragmentation patterns. Samples included malto-oligosaccharides, high-mannose type *N*-linked glycans released from ribonuclease B and asialo- and disialylated-biantennary *N*-linked complex glycans from various sources.

Materials and Methods

Malto-oligosaccharides, the permethylation reagents dimethyl sulfoxide, sodium hydroxide, and methyl

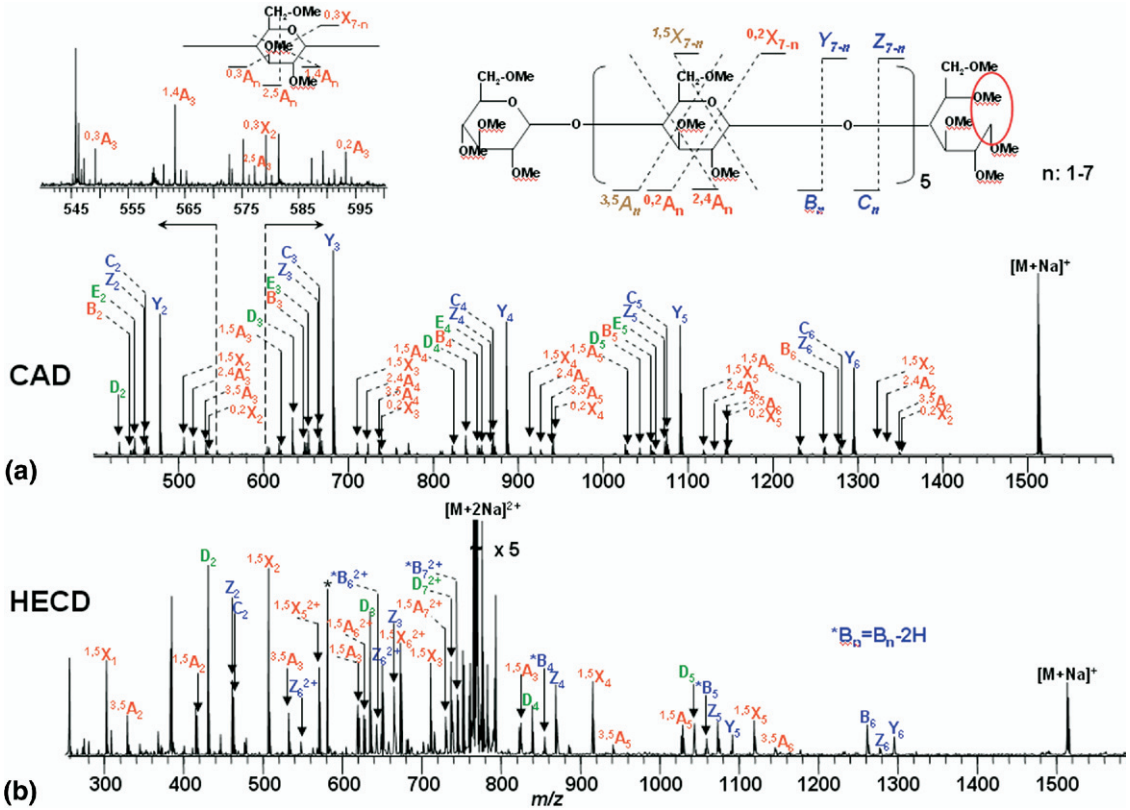

Figure 1. (**a**) CAD MS/MS spectrum of reduced and permethylated maltoheptaose $[M + 2Na]^{2+}$ *m/z* 768.376. The internal fragments labeled with ^ are B/Y cleavages and the internal fragments labeled with the number symbol are C/Y cleavages. (*b*) "Hot" ECD MS/MS spectrum of reduced and permethylated maltoheptaose $[M + 2Na]^{2+}$ *m/z* 768.376. The peak labeled with an asterisk indicates electronic noise. All the fragment ions are sodiated except those labeled with (H). The masses and assignments of these peaks are available in Supplemental Tables S1 and S2. Glycosidic cleavages are labeled in blue, cross-ring cleavages are labeled in red, internal fragments are labeled in green.

iodide as well as chloroform and other solvents, and the reducing reagent sodium cyanoborohydride were obtained from Sigma-Aldrich (St. Louis, MO). Ribonuclease B and glycerol-free PNGase F were obtained from New England Biolabs Inc. (Beverly, MA). Asialo and disialylated biantennary complex *N*-linked glycans were obtained from CalBiochem (San Diego, CA).

Sample Preparation

All native glycans, malto-oligosaccharides, including the maltoheptaose that was reduced by sodium cyanoborohydride [80], high-mannose type *N*-linked glycans released from ribonuclease B by PNGase F, and the commercial samples of asialo and disialylated biantennary complex *N*-linked glycans, were dissolved in Me_2SO and per-*O*-methylated by treating with powdered sodium hydroxide with methyl iodide using the method introduced by Ciucanu and Kerek [81] as modified by Ciucanu and Costello [82]. The purified and dried samples were dissolved in 60/40 (25 mM aqueous NaOH)/(50% aqueous methanol) to a concentration of ~5–10 pmol/μL solution.

FTMS Instrumentation

A custom-built qQq-FT mass spectrometer with a nanospray source and 7T actively shielded magnet (Cryomagnetics Inc., Oak Ridge, TN) was utilized in this study [6, 22]. The "qQq" front-end encompasses a focusing rf-only quadrupole (Q0), followed by a resolving quadrupole (Q1), and a LINAC quadrupole collision cell (Q2) [83, 84]. Ions can be isolated in the mass resolving Q1 and accumulated in Q2 before analysis in the ICR cell. The instrument was designed to employ several fragmentation methods, including Q2 collisionally activated dissociation (Q2 CAD) [6, 21, 22], electron capture dissociation (ECD) [26–28], and sustained off-resonance irradiation (SORI) CAD [23, 24]. The front-end quadrupoles were controlled using the program LC2Tune 1.5 (MDS SCIEX, Toronto, Canada), and the program IonSpec99 (IonSpec, Lake Forest, CA) controlled data acquisition in the ion cyclotron-resonance (ICR) cell. For each analysis, the solution of permethylated oligosaccharide (~2–3 μL) was loaded into a glass capillary tip pulled with a micropipette puller (model P-97; Sutter Instruments Co., Novato, CA) to ~1 μm orifice diameter, and a stainless steel wire was inserted

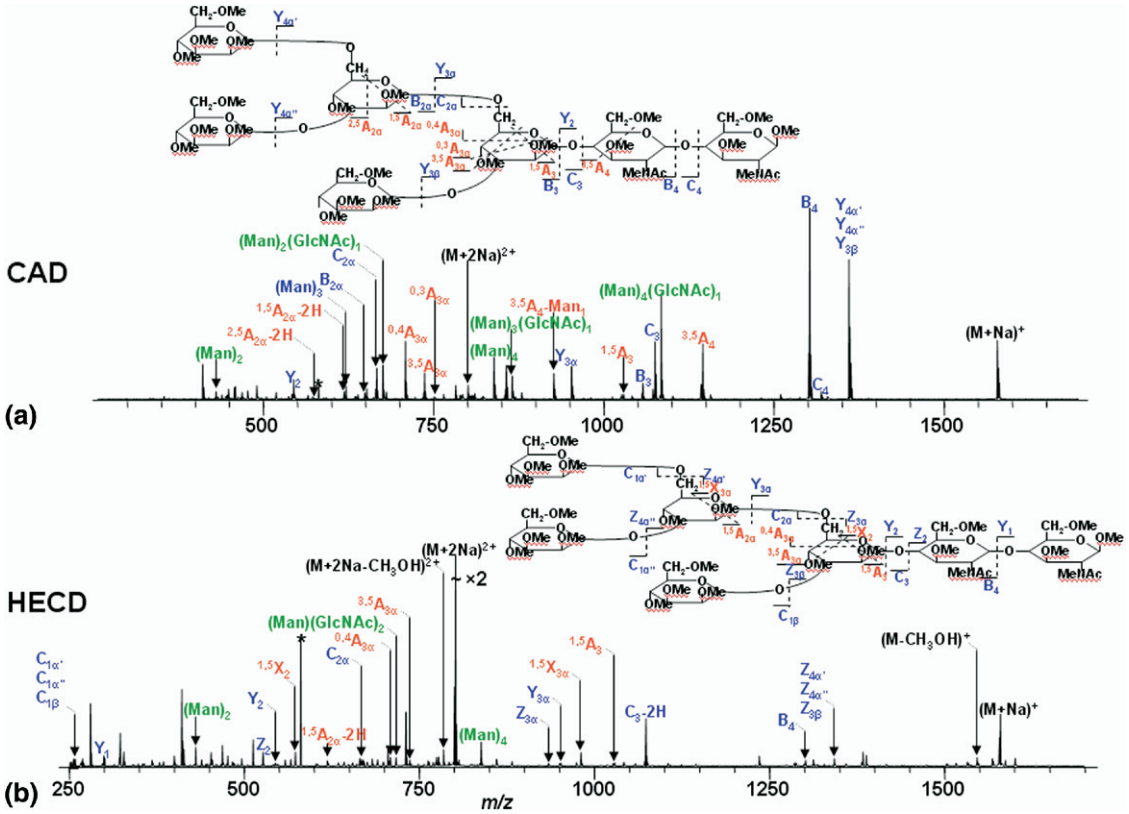

Figure 2. (**a**) CAD MS/MS spectrum of permethylated $GlcNAc_2Man_5$ $[M + 2Na]^{2+}$ *m/z* 801.386. (**b**) "Hot" ECD MS/MS spectrum of permethylated $GlcNAc_2Man_5$ $[M + 2Na]^{2+}$ *m/z* 801.386. All the fragment ions are sodiated except the ones labeled with (H). The peaks labeled with (2Na) are two sodiated ions. The subscript x means α' or α'', or β. The masses and assignments of these peaks are available in Supplemental Tables S4 and S9. Glycosidic cleavages are labeled in blue, cross-ring cleavages are labeled in red, internal fragments are labeled in green.

into the distal end of the tip to form the electrical connection. For Q2CAD experiments, the parent ions were isolated by Q1, and were fragmented by low-energy (40–80 eV) collisions with N_2 gas in Q2. For "hot" ECD experiments, the parent ions were isolated in Q1 and externally accumulated in Q2 for 1000–2500 ms. After being transferred and trapped in the cylindrical ICR cell, ions were irradiated with 5-14 eV electrons from a 1.2 A heated dispenser cathode [85] for 200 to 1000 ms and were fragmented. The total pulse duration for CAD and ECD experiments varied between 1000 ms and 5000 ms and all data were analyzed without apodization and with two zerofills to improve mass accuracy. Other experimental parameters were reported previously [6, 7, 22].

Results and Discussion

Sodiated and Permethylated Linear Malto-oligosaccharides

The sodiated $[M + 2Na]^{2+}$ molecular ions corresponding to each of the permethylated linear malto-oligosaccharide samples $(Glc)_6$–$(Glc)_9$ were detected by ESI-FTMS. For each sample, the peak indicating the doubly charged sodiated molecular ion was isolated in Q1 and fragmented by Q2 CAD. The fragmentation patterns of $(Glc)_6$–$(Glc)_9$ are very similar to one another; the maltoheptaose $(Glc)_7$ spectrum is shown as an example in Supplemental Figure S2. Three types of product ions, those resulting from glycosidic cleavages (B, Y, C, and Z ions), cross-ring cleavages (A and X ions), and internal cleavages (fully glycosidic, e.g., B/Y, C/Y, and mixed glycosidic and cross-ring cleavages, e.g., A/Y, B/X ions) were all observed in these spectra. Due to the high symmetry of linear malto-oligosaccharides, B_n and Z_n, C_n and Y_n, $^{0,2}X_n$ and $^{2,4}A_{n+1}$ ions are isobaric. To differentiate them, the maltoheptaose was reduced by sodium cyanoborohydride. Figure 1 illustrates the MS/MS spectra (CAD and "hot" ECD) of permethylated reduced maltoheptaose. Extensive fragmentation was detected in the CAD experiment, and Y ions were the most abundant type of product ions. Consecutive Y_6 to Y_2 ions defined the masses of the fragment ion series and the 204.0998 Da mass increment between sequential members of this series of high abundance peaks corresponds to the mass of the permethylated hexose units that form the oligosaccharide. The C/Y internal fragment ions with loss of methanol ($^{\#}(Glc)_n$-CH_3OH) are

Table 1. CAD fragment ions observed from permethylated high mannose glycans

			Man7				
	Man5	Man6	Isomer1	Isomer2	Isomer3	Man8	Man9
Glycosidic cleavages	Y_2; $Y_{3\alpha}$; $Y_{4\alpha' \text{ or } 4\alpha'' \text{ or } 4\beta}$; $B_{2\alpha}$; B_3; B_4 $C_{2\alpha}$; C_3; C_4	Y_2; $Y_{3\alpha}$; $Y_{3\beta}$; $Y_{4\alpha' \text{ or } 4\alpha'' \text{ or } 4\beta}$; $B_{2\alpha}$; $B_{2\beta}$; B_3; B_4 $C_{2\alpha}C_{2\beta}$; C_3; C_4	Y_2; $Y_{3\alpha \text{ or } 3\beta}$; $Y_{4\beta}$; $Y_{4\alpha' \text{ or } 4\alpha'' \text{ or } 5\beta}$; $B_{2\beta}$; B_5; $B_{2\alpha \text{ or } 3\beta}$ $C_{2\alpha \text{ or } 3\beta}$; $C_{2\beta}$; C_4	Y_2; $Y_{3\alpha}$; $Y_{\beta 4\alpha' \text{ or } 3\beta}$; $Y_{5\alpha' \text{ or } 4\alpha'' \text{ or } 4\beta}$; $B_{2\alpha' \text{ or } 2\beta}$; $B_{3\alpha}$; B_5 $C_{2\alpha' \text{ or } 2\beta}$; $C_{3\alpha}$; C_4; $W_{2\alpha'}$	$Y\beta_2$; $Y_{3\alpha}$; $Y_{4\alpha' \text{ or } 5\alpha'' \text{ or } 4\beta}$; $Y_{4\alpha'' \text{ or } 3\beta}$; $B_{2\alpha'' \text{ or } 2\beta}$; $B_{3\alpha}$; B_5 $C_{2\alpha'' \text{ or } 2\beta}$; $C_{3\alpha}$; C_4	Y_2; $Y_{3\alpha}$; $Y_{3\beta}$; $Y_{4\alpha' \text{ or } 4\beta}$; $Y_{5\alpha' \text{ or } 4\alpha'' \text{ or } 5\beta}$; $B_{2\alpha' \text{ or } 2\beta}$; $B_{3\alpha}$; $B_{3\beta}$; B_5 $C_{2\alpha' \text{ or } 2\beta}$; $C_{3\alpha}$; $C_{3\beta}$	Y_2; $Y_{3\alpha}$; $Y_{3\beta}$; $Y_{4\alpha' \text{ or } 4\alpha'' \text{ or } 4\beta}$; $Y_{5\alpha' \text{ or } 5\alpha'' \text{ or } 5\beta}$; $B_{2\alpha' \text{ or } 2\alpha'' \text{ or } 2\beta}$; $B_{3\alpha}$; $B_{3\beta}$; B_5 $C_{2\alpha' \text{ or } 2\alpha'' \text{ or } 2\beta}$; $C_{3\alpha}$; $C_{3\beta}$; C_5
Cross ring cleavages	$^{0,4}A_{3\alpha}$; $^{3,5}A_{3\alpha}$; $^{3,5}A_4$; $^{2,5}A_{2\alpha}$-2H; $^{1,5}A_{2\alpha}$-2H; $^{1,5}A_3$; $^{0,3}A_{3\alpha}$	$^{0,4}A_{3\alpha}$; $^{3,5}A_{3\alpha}$; $^{3,5}A_4$ $^{1,5}A_{2\alpha}$-2H	$^{0,4}A_{3\alpha}$; $^{3,5}A_{3\alpha}$; $^{2,4}A_{4\beta}$ or $^{1,3}A_{4\beta}$	$^{0,4}A_{3\alpha}$; $^{0,4}A_{4\alpha}$; $^{3,5}A_{4\alpha}$	$^{0,4}A_{4\alpha}$; $^{3,5}A_{4\alpha}$	$^{0,4}A_{3\alpha}$; $^{0,4}A_{4\alpha}$; $^{3,5}A_{4\alpha}$; $^{1,5}A_{3\beta}$; $^{2,4}A_{4\beta}$ or $^{1,3}A_{4\beta}$ $^{1,3}A_{3\beta}$	$^{0,4}A_{3\alpha}$; $^{0,4}A_{4\alpha}$; $^{3,5}A_{3\alpha}$; $^{3,5}A_{4\alpha}$; $^{1,5}A_{2\alpha' \text{ or } 2\alpha'' \text{ or } 2\beta}$; $^{1,5}A_{3\beta}$; $^{2,4}A_{3\alpha'' \text{ or } 3\beta}$ or $^{1,3}A_{3\alpha''}$; $^{2,4}A_{4\beta}$ or $^{1,3}A_{4\beta}$
Internal fragments	$(Man)_{2-4}$; $(Man)_{2-4}GlcNAc$	$(Man)_{3-5}$; $(Man)_{3-4}GlcNAc$	$(Man)_{2-6}$; $(Man)_{3-6}GlcNAc$			$(Man)_{2-6}$; $(Man)_{3-7}GlcNAc$	$(Man)_{2-6}$; $(Man)_{4-6}GlcNAc$

Man7 Isomer 1

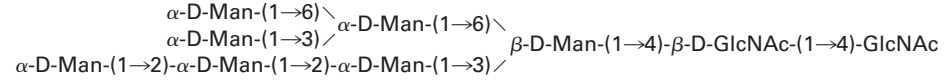

Man7 Isomer 2

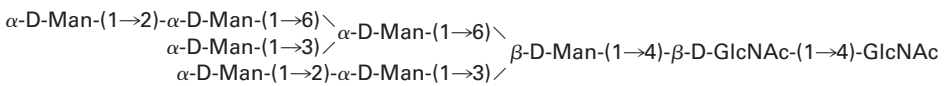

Man7 Isomer 3

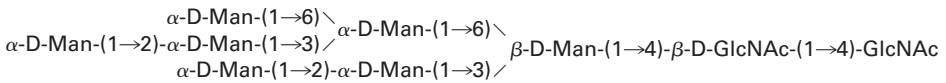

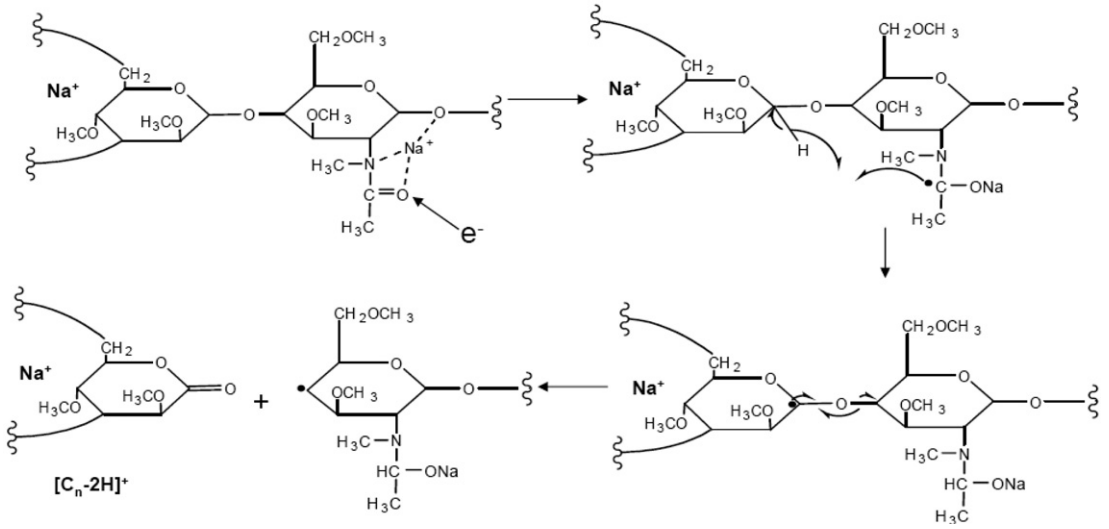

Scheme 1

similar in mass to $^{1,5}A_n$, for example, the mass of $^{\#}(Glc)_3$-CH_3OH is 621.2735 and the mass of $^{1,5}A_3$ is 621.3100, but they are easily differentiated by FTMS (Figure 1a inset). "Hot" ECD provided cleavages similar to CAD but fewer peaks resulted from cross-ring cleavages. These data agree with a previous report on similar studies on linear oligoglycosamides and oligoglycosamines, which compared EID with ECD and CAD [73], although likely the EID experiments reported also showed considerable electron capture, as evidenced by the presence of odd-electron fragments.

Sodiated and Permethylated High-Mannose Type N*-linked Glycans*

Ribonuclease B is a 15-kDa protein, with a heterogeneous, high mannose glycan, $GlcNAc_2Man_{5-9}$ (GlcNAc = *N*-acetylglucosamine, Man = mannose), attached to Asn34. The high-mannose glycans ($GlcNAc_2Man_{5-9}$) were released from ribonuclease B by PNGase F and permethylated. The $[M + 2Na]^{2+}$ sodiated doubly charged molecular ions from $GlcNAc_2Man_5$ to $GlcNAc_2Man_9$ were individually isolated and fragmented in separate CAD and "hot" ECD experiments (Supplemental Figures S3 and S4). Fu et al. [86] have investigated the structures of all the high-mannose glycan released from ribonuclease B (Supplemental Figure S5) by ^1H NMR and time-of-flight mass spectrometry and determined that the single isomer of $GlcNAc_2Man_5$ accounts for 57% of the mixture. Our result is consistent with their research and also indicated that the $GlcNAc_2Man_5$ glycoform has the highest abundance for ribonuclease B. Figure 2 shows the CAD and "hot" ECD mass spectra of permethylated $GlcNAc_2Man_5$. In the CAD spectrum (Figure 2a), B and Y ions are the major products from glycosidic cleavage and A-type ions are the major products from cross-ring cleavage. The last series ($^{0,4}A_{3\alpha}$, $^{3,5}A_{3\alpha}$, and $^{0,3}A_{3\alpha}$) show that the linkage position of the major branch is at the 6-position of the central core mannose residue. The B_4 fragment, arising from cleavage within the core chitobiose, is the most abundant B-ion, in agreement with results obtained by Harvey et al. in high-energy CAD experiments [51]. In addition, many abundant internal fragment ions, which provide the branch composition information, were observed. The loss of terminal mannose residues was always detected in CAD spectra. The $GlcNAc_2Man_{6-9}$ fragmentation patterns are similar to those of $GlcNAc_2Man_5$. Table 1 lists all the CAD fragmentation ions observed for $GlcNAc_2Man_{5-9}$; the calibrated masses of these observed peaks are available in Supplementary Tables S4–S8. All tables contain the masses of all observed monoisotopic peaks and the assignments of those that could be determined. Unassigned peaks could be due to additional isomers or rearrangements that occur prior or during fragmentation. B, Y, and a few C ions constitute the major series of glycosidic fragment ions; A-type ions are the most important cross-ring fragment ions, especially because the $^{0,4}A_n$ and $^{3,5}A_n$ ions provide branching and linkage information. Internal fragments including $(Man)_x$ and $(Man)_yGlcNAc$ cleaved from two terminals also helped to determine the branching patterns. For example, x is 3–5 and y is 3–4 for the fragments observed in the spectrum of the $GlcNAc_2Man_6$ sample. $GlcNAc_2Man_6$ and $GlcNAc_2Man_8$ each have one dominant isomer, although other isomers exist in the sample released from ribonuclease B. $GlcNAc_2Man_7$, however, has three isomers that have similar relative abundances and all three isomers were detected in the sample by mass spectrometry. The fragment $^{0,4}A_{3\alpha}$ (709.3257 Da) indicated the presence of isomer 1 (Table 1) while $^{0,4}A_{4\alpha}$ (913.4249 Da) provided evidence for the presence of isomer 2 and/or 3 (Table 1).

Like the CAD spectrum, the "hot" ECD spectrum of the $GlcNAc_2Man_5$ doubly charged sodiated molecular ion

Table 2. ECD fragment ions observed from permethylated high mannose glycans

			Man7				
	Man5	Man6	Isomer1	Isomer2	Isomer3	Man8	Man9
Glycosidic cleavages	$C_{1\alpha'\text{ or }1\alpha''\text{ or }1\beta}$; $C_{2\alpha}$; C_3-2H; C_4-2H(2Na) Z_2; $Z_{3\alpha}$; $Z_{4\alpha'\text{ or }4\alpha''\text{ or }3\beta}$; Y_1; Y_2; $Y_{3\alpha}$; $Y_{4\alpha'\text{ or }4\alpha''\text{ or }3\beta}$(2Na) B_4	$C_{1\alpha'\text{ or }1\alpha''\text{ or }1\beta}$; $C_{2\alpha}$-2H; $C_{2\beta}$-2H; C_3; C_4-2H Z_2; $Z_{3\beta}$; $Z_{4\alpha'\text{ or }4\alpha''\text{ or }4\beta}$ Y_1; Y_2; $Y_{3\alpha}$(2Na); $Y_{3\beta}$(2Na); $Y_{4\alpha'\text{-2H or }4\alpha''\text{-2H or }4\beta\text{-2H}}$ $B_{2\alpha}$; $B_{2\beta}$; B_4	$C_{2\alpha}$-2H; $C_{2\beta}$-2H; C_4-2H; Z_2	$C_{2\alpha'\text{ or }2\beta}$-2H; C_4-2H; Z_2	$C_{2\alpha'\text{ or }2\beta}$-2H; C_4-2H; Z_2	$C_{2\alpha'\text{ or }2\beta}$-2H; C_4-2H; Z_2	$C_{3\alpha}$; $C_{3\beta}$-2H; C_4-2H; Z_2
Cross ring cleavages	$^{0,4}A_{2\alpha'}$(2Na); $^{0,4}A_{3\alpha}$; $^{3,5}A_{3\alpha}$; $^{3,5}A_5$-H $^{1,5}A_{2\alpha}$-2H; $^{1,5}A_3$; $^{1,5}A_5$-H $^{1,4}A_4$-2H(2Na) $^{1,5}X_1$; $^{1,5}X_2$; $^{1,5}X_{3\alpha}$; $^{1,5}X_{4\alpha'\text{ or }4\alpha''}$	$^{0,4}A_{2\alpha'}$(2Na); $^{0,4}A_{3\alpha}$; $^{3,5}A_{3\alpha}$ $^{1,5}A_{2\alpha}$-2H; $^{1,5}A_{2\beta}$; $^{1,5}A_3$; $^{1,5}A_5$-2H $^{2,4}A_{2\alpha''}$; $^{2,4}A_{3\beta}$ or $^{1,3}A_{3\beta}$ $^{1,5}X_1$; $^{1,5}X_2$; $^{1,5}X_{3\alpha}$; $^{1,5}X_{3\beta}$; $^{1,5}X_{4\alpha'\text{ or }4\alpha''\text{ or }4\beta}$					
Internal fragments	$(Man)_{2-4}$; $(Man)(GlcNAc)_2$	$(Man)_{2-5}$; $(Man)(GlcNAc)_2$					

Man7 Isomer 1

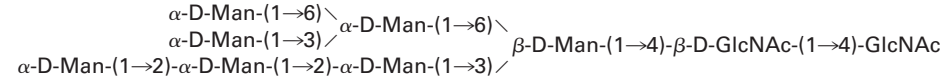

Man7 Isomer 2

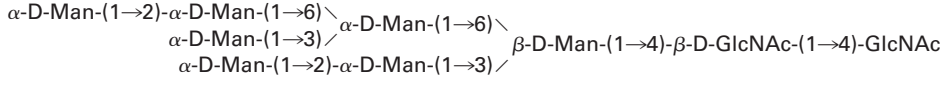

Man7 Isomer 3

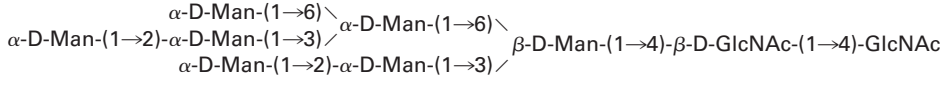

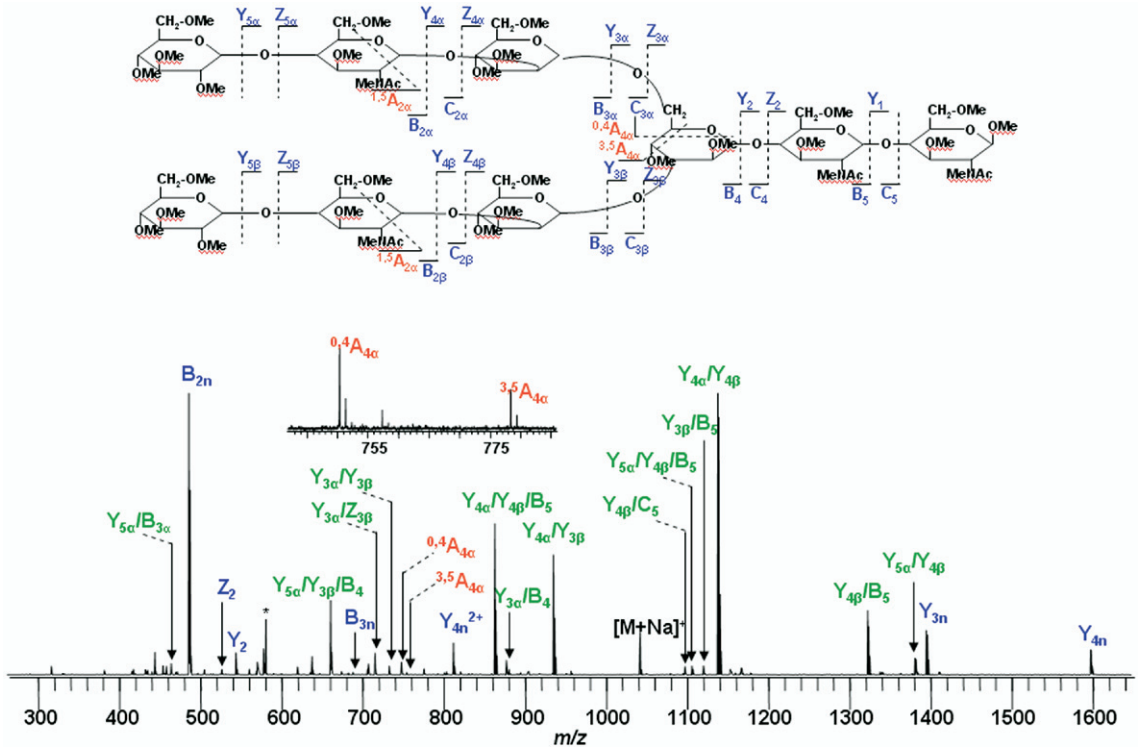

Figure 3. CAD MS/MS spectrum of a permethylated asialo-biantennary *N*-linked glycan $[M + 2Na]^{2+}$ *m/z* 1046.513. The cartoon structure shows observed cleavages and the inset shows an expansion of the region *m/z* 743–785. The peaks labeled with filled diamonds indicate that only one of several possible internal fragments is shown. The subscript x means α or β. The masses and assignments of these peaks are available in Supplemental Table S11. Glycosidic cleavages are labeled in blue, cross-ring cleavages are labeled in red, internal fragments are labeled in green.

(Figure 2b) included glycosidic, cross-ring, and internal cleavages. C and Z ions are the most abundant glycosidic fragments and some C-2H ions also exist. For example, the C_3-2H ion is abundant, which was also observed for a series of C_n-2H ions in the "hot" ECD spectra of complex *N*-linked glycans (asialo- and disialylated biantennary *N*-linked glycans, Figure 4 and Figure 6). In each case, the abundant C_n-2H ions are observed next to a GlcNAc residue, which can be explained by Scheme **1**. Complementary X-type cross-ring fragments were observed in the "hot" ECD spectrum. The presence of these fragments establishes the sequence, branching pattern, and linkage information. Internal fragment ions were also observed, but fewer than were present in the CAD spectrum. Some secondary fragment ions and losses that could be correlated with the loss of small, even and odd electron neutral fragments were also detected. As shown in Table 2, ECD of $GlcNAc_2Man_6$ generated a fragmentation pattern similar to that of $GlcNAc_2Man_5$ but the ECD efficiency was relatively low for the $[M + 2Na]^{2+}$ doubly charged sodiated molecular ions of $GlcNAc_2Man_7$, $GlcNAc_2Man_8$, and $GlcNAc_2Man_9$, and few C and Z ions were detected. This low efficiency correlates well with observed trends in peptides and is likely due to a combination of factors. First, ECD efficiency typically scales with the square of the charge state. Second, ECD efficiency is usually lower for larger molecules due to increased intramolecular noncovalent bonding that prevents fragments from separating. Third, heterogeneity in the isomers (as is known in $GlcNAc_2Man_7$) would result in a greater distribution of lower abundance fragment ions. Overall, CAD and "hot" ECD experiments on high-mannose type glycans were complementary since B and Y ions were detected in CAD while C and Z ions were detected in "hot" ECD. In addition, some complementary A- and X-type cross-ring cleavages were observed in the "hot" ECD spectra of $GlcNAc_2Man_{5-6}$. C/Z ions provide similar structural information to the B/Y ions, but the two ion pairs together provide the additional information of the directionality of the cleavages, similar to the complementary "golden pairs" observed in CAD/ECD of proteins [87].

Sodiated and Permethylated Complex N-Linked Glycans

The CAD and "hot" ECD experiments were performed on the $[M + 2Na]^{2+}$ doubly charged sodiated molecular ion of a permethylated asialo-biantennary *N*-linked glycan (Figure 3 and 4). In the CAD spectrum (Figure 3), extensive and abundant internal fragment ions were detected in addition to B, Y, and A ions. Although these fragments provide sequence and branching information, the existence of many internal fragment ions complicates the

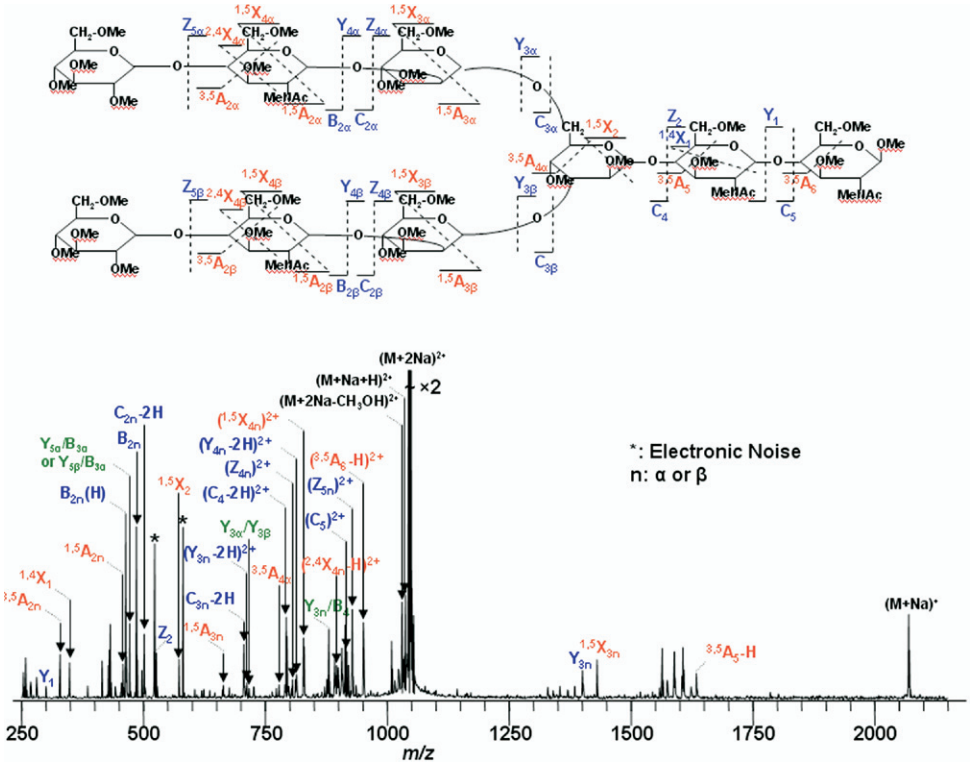

Figure 4. "Hot" ECD MS/MS spectrum of a permethylated asialo-biantennary *N*-linked glycan $[M + 2Na]^{2+}$ *m/z* 1046.513. The cartoon structure shows observed cleavages. The peaks labeled with asterisks indicate electronic noise. The subscript x means α or β. All the fragment ions are sodiated except the ones labeled with (H). The masses and assignments of these peaks are available in Supplemental Table S12. Glycosidic cleavages are labeled in blue, cross-ring cleavages are labeled in red, internal fragments are labeled in green.

spectral interpretation due to multiple possibilities for some masses $^{0,4}A_{4\alpha}$ and $^{3,5}A_{4\alpha}$ ions determine the linkage position of the branch to be at the 6-position of the central core mannose residue and confirm the branching composition. Compared with the CAD spectrum, the "hot" ECD spectrum of this glycan provides more structural information. More cross-ring fragment ions were observed in the "hot" ECD spectrum and most of the A ions were accompanied by complementary X ions. C and Z ions were the major glycosidic fragments detected in the "hot" ECD spectrum and fewer internal fragment ions were present compared with the CAD spectrum. Although the number of monosaccharide units is the same as $GlcNAc_2Man_7$, the "hot" ECD fragment coverage is much higher. Some abundant fragment ions in the spectrum, notably the cluster at *m/z* 1550–1625 are as yet unexplained, and hence marked with a "?". Additional research into the mechanism of fragmentation of these molecules is ongoing in an attempt to assign them.

Finally, CAD and "hot" ECD spectra of a permethylated disialylated-biantennary *N*-linked glycan were generated. Higher collision energy (60 eV versus 80 eV) was required to fragment sialylated glycans to the same extent as their asialo analogs, probably due to the presence of additional noncovalent interactions which stabilize the molecule. ESI of the permethylated glycans avoided the extensive loss of sialic acids observed in the MALDI mass spectra of native sialylated glycans [88–91]. The methyl esterification that is introduced during permethylation blocks the destabilizing interaction of the carboxyl group with the adjacent glycosidic linkage and therefore reduces desialylation. In the CAD experiment (Figure 5), the $[M + 2Na]^{2+}$ doubly charged sodiated molecular ion was isolated and fragmented and the fragmentation pattern was similar as that of the asialo-biantennary *N*-linked glycan (Figure 3). Some B, Y, and A ions were detected but extensive and abundant internal fragment ions were also observed.

The "hot" ECD spectrum on this doubly charged disialylated glycan was not useful due to low ECD efficiency. However, the larger complex glycans, including the sialylated glycans, in particular, often generate abundant peaks having higher charge states. In this case, the $[M + 3Na]^{3+}$ triply charged sodiated molecular ion was relatively abundant and "hot" ECD on this ion resulted in extensive fragmentation (Figure 6) providing much more structural information than did CAD. In addition to C, Z, and some B, Y glycosidic fragmentation ions, the products of many complementary A- and X-type cross-ring cleavages were observed, and these confirmed the sequence and branching linkages of this glycan. Interestingly, the B_1^+ ion (B_1{H} in

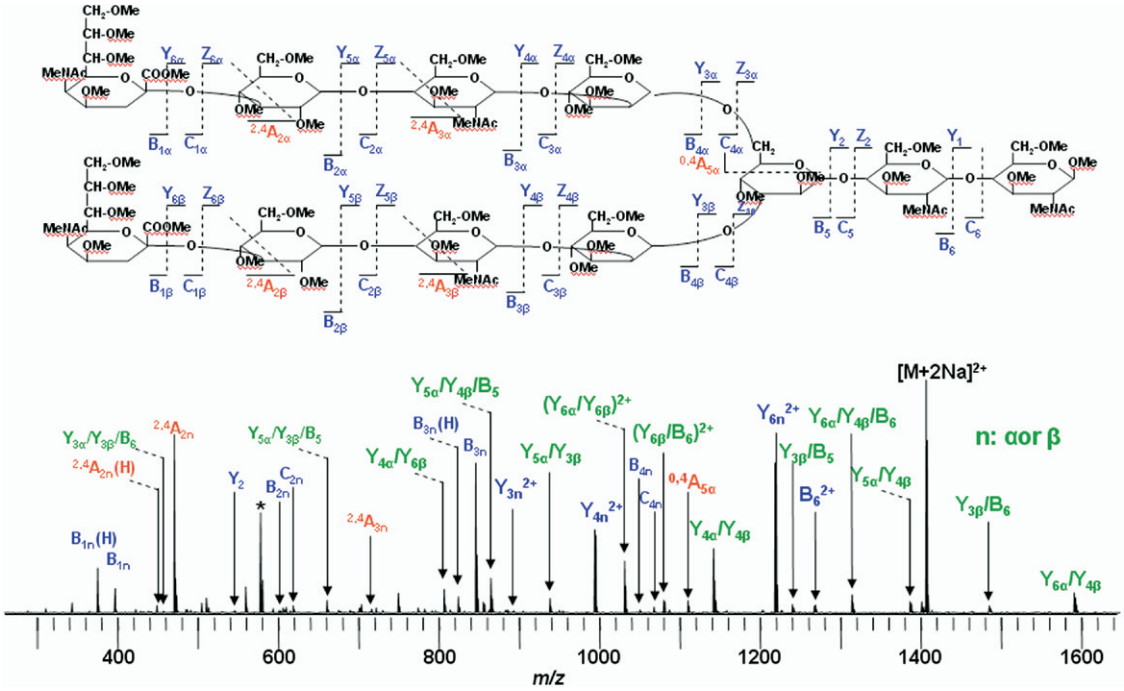

Figure 5. CAD MS/MS spectrum of a permethylated disialylated-biantennary *N*-linked glycan $[M + 2Na]^{2+}$ *m/z* 1407.686. The cartoon structure shows observed cleavages. The peaks labeled with asterisks indicate electronic noise. All the fragment ions are sodiated except the ones labeled with (H). The peaks labeled with filled diamonds mean only one of several possible internal fragments is listed. The subscript x means α or β. The masses and assignments of these peaks are available in Supplemental Table S13. Glycosidic cleavages are labeled in blue, cross-ring cleavages are labeled in red, internal fragments are labeled in green.

Figure 6) was noticeably abundant in the sialylated glycan; this fragment ion has no sodium adducts, which is surprising since the precursor ion was $[M + 3Na]^{3+}$. A possible mechanism for formation of this ion is shown in Scheme **2**. Also, the $^{0,4}A_{5\alpha}$ ion confirmed the branch linkage position. In addition, the successive $^{1,5}X_{5\alpha/\beta}$, $^{1,5}X_{4\alpha/\beta}$, $^{1,5}X_{3\alpha/\beta}$ confirmed the redundant sequences of the two branches.

Few papers have discussed ECD of sodiated peptide or glycan ions [73, 92, 93]. Hudgins et al. showed that ECD on peptides bearing alkali attachments (Na^+ or K^+) or fixed-charges generated alkali-attached and fixed-charge analogs of the c and z ions formed from the protonated peptides, and the authors proposed that N–C_α bonds were cleaved by direct dissociative electron attachment [92]. Williams and coworkers performed ECD on cationized peptides $[M + 2Li]^{2+}$ and $[M + 2Cs]^{2+}$ to produce di- and monometalated analogs of the same c and z ions observed from the $[M + 2H]^{2+}$ [93]. In our study, all the "hot" ECD experiments were performed on di- or trisodiated molecular ions and the unstable, charge-reduced molecular ions $[M + 2Na]^{2+\cdot}$ or $[M + 3Na]^{3+\cdot}$ were not detected, although relatively abundant $[M + Na]^+$ or $[M + 2Na]^{2+}$ ions were observed and can be formed by loss a neutral sodium atom from the charge-reduced molecular ions. Most of the fragment ions (C, Z, cross-ring, and internal fragment ions) observed were sodiated except for a couple of B(H) and A(H) ions detected in the spectra of asialo- and disialylated-biantennary *N*-linked glycans. Such behavior is also observed in the high- and low-energy CAD spectra of permethylated glycans and glycoconjugates.

Saccharide rearrangements happen often during MS/MS experiments on protonated oligosaccharides and glycoconjugates [57]. However, these rearrangements are blocked by permethylation and/or cationization, consistent with the data shown herein. Glycan rearrangements have previously been observed for ECD of glycosaminoglycans (I. Jonathan Amster, personal communication), which are not candidates for permethylation because the derivatization conditions would cause loss of the sulfate groups, whose numbers and locations need to be preserved and determined to establish structure/activity relationships.

Conclusions

CAD and "hot" ECD tandem mass spectrometry were utilized in this research to analyze the structures of glycans following their permethylation. Linear maltooligosaccharides ($\{Glc\}_6$-$\{Glc\}_9$) generated similar fragment patterns in CAD and "hot" ECD. B, Y, C, and Z glycosidic ions, A and X cross-ring ions and B/Y and C/Y type internal ions were all observed and could be

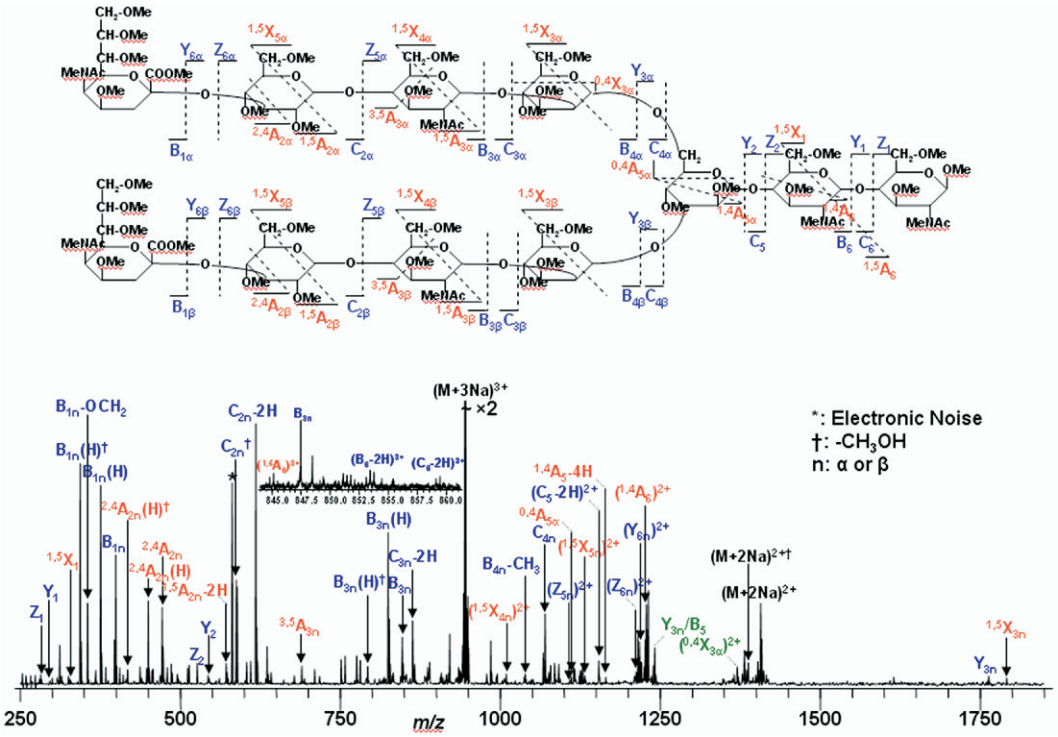

Figure 6. "Hot" ECD MS/MS spectrum of a permethylated disialylated-biantennary *N*-linked glycan $[M + 3Na]^{3+}$ *m/z* 946.121. The cartoon structure shows observed cleavages. The peaks labeled with asterisks indicate electronic noise. The peaks labeled with daggers indicate loss of CH_3OH. The subscript x means α or β. The inset shows an expansion of the region *m/z* 845–860. All the fragment ions are sodiated except the ones labeled with (H). The masses and assignments of these peaks are available in Supplemental Table S14. Glycosidic cleavages are labeled in blue, cross-ring cleavages are labeled in red, internal fragments are labeled in green.

used to sequence the oligosaccharides. In contrast to results obtained for the linear malto-oligosaccharides, CAD and "hot" ECD experiments performed on branched *N*-linked glycans provided complementary structural information. The sequence information available for these glycans was confirmed by B, Y ions in CAD and C, Z ions in "hot" ECD. The branching patterns were determined by cross-ring cleavages (A-type in CAD and complementary A and X pairs in "hot" ECD). Internal fragments are particularly frequent in CAD spectra but also occur in ECD spectra. The linkage information for the branches was obtained from $^{0,4}A$ and $^{3,5}A$ ions. In agreement with the literature [75], higher collision energy was required to fragment permethylated sialylated glycans to the same extent as their asialo counterparts, which is, perhaps, surprising since the previous work was for negative ions, [75] where it is not clear a priori, that the mechanism is the same. The triply charged $[M + 3Na]^{3+}$ molecular ion of the permethylated disialylated-biantennary *N*-linked

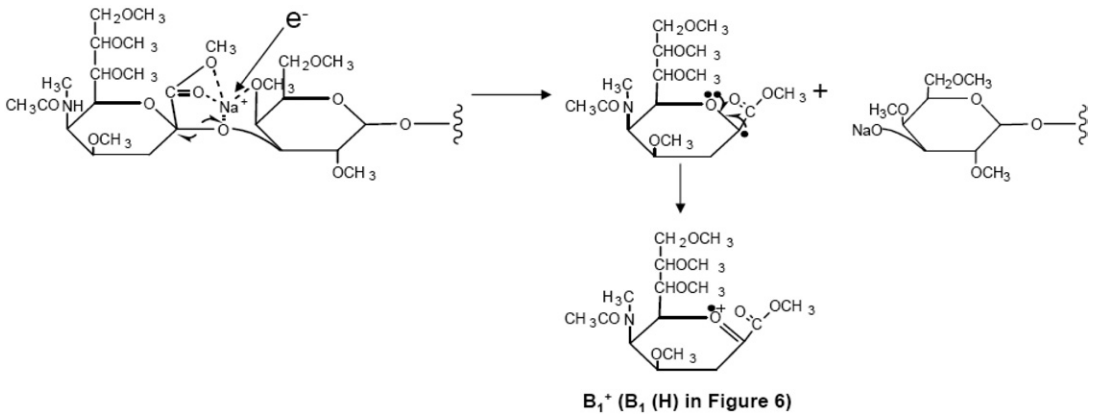

Scheme 2

glycan was abundant and was fragmented by the "hot" ECD experiment, generating extensive product ions (glycosidic and complementary pairs resulting from cross-ring cleavages) to fully confirm the sequence, branching, and linkage information of this glycan. Fragmentation of the larger high-mannose type glycans, such as $GlcNAc_2Man_{7-9}$, by ECD is still difficult but may be improved by activated ion ECD [94].

Acknowledgments

The authors thank Jason J. Cournoyer, Dr. Cheng Lin, Professor Joseph Zaia, and Professor John Cipollo for valuable suggestions. This research was supported by NIH P41-RR10888, N01-HV28178, Petroleum Research Fund, and MDS SCIEX.

References

1. Karlsson, K. A. Animal Glycosphingolipids as Membrane Attachment Sites for Bacteria. *Annu. Rev. Biochem.* **1989,** *58,* 309–350.
2. Varki, A. Biological Roles of Oligosaccharides—All of the Theories are Correct. *Glycobiology* **1993,** *3,* 97–130.
3. Sturgeon, R. J. Carbohydrate Chemistry; Oxford Science Publications: Oxford, 1988.
4. Treuheit, M. J.; Costello, C. E.; Halsall, H. B. Analysis of the 5 Glycosylation Sites of Human α-1-Acid Glycoprotein. *Biochem. J.* **1992,** *283,* 105–112.
5. Treuheit, M. J.; Costello, C. E.; Kirley, T. L. Structures of the Complex Glycans Found on the β-Subunit of (Na,K)-Atpase. *J. Biol. Chem.* **1993,** *268,* 13914–13919.
6. O'Connor, P. B., Pittman, J. L., Thomson, B. A., Budnik, B. A., Cournoyer, J. C., Jebanathirajah, J., Lin, C., Moyer, S., Zhao, C. A New Hybrid Electrospray Fourier Transform Mass Spectrometer: Design and Performance Characteristics. *Rapid Commun, Mass Spectrom,* **2006,** *20,* 259–266.
7. Zhao, C.; Sethuraman, M.; Clavreul, N.; Kaur, P.; Cohen, R. A.; O'Connor, P. B. Detailed Map of Oxidative Post-Translational Modifications of Human P21Ras Using Fourier Transform Mass Spectrometry. *Anal. Chem.* **2006,** *78,* 5134–5142.
8. Gage, D. A.; Rathke, E.; Costello, C. E.; Jones, M. Z. Determination of Sequence and Linkage of Tissue Oligosaccharides in Caprine β-Mannosidosis by Fast-Atom-Bombardment Collisionally Activated Dissociation Tandem Mass-Spectrometry. *Glycoconj. J.* **1992,** *9,* 126–131.
9. Jones, M. Z.; Rathke, E. J. S.; Gage, D. A.; Costello, C. E.; Murakami, K.; Ohta, M.; Matsuura, F. Oligosaccharides Accumulated in the Bovine β-Mannosidosis Kidney. *J. Inherit. Metab. Dis.* **1992,** *15,* 57–67.
10. Costello, C. E., Contado-Miller, J. M., Cipollo, J. F. A Glycomics Platform for the Analysis of Permethylated Oligosaccharide Alditols. Unpublished.
11. Fenn, J. B.; Mann, M.; Meng, C. K.; Wong, S. F.; Whitehouse, C. M. Electrospray Ionization for Mass-Spectrometry of Large Biomolecules. *Science* **1989,** *246,* 64–71.
12. Karas, M.; Hillenkamp, F. Laser Desorption Ionization of Proteins with Molecular Masses Exceeding 10,000 Daltons. *Anal. Chem.* **1988,** *60,* 2299–2301.
13. Hillenkamp, F.; Karas, M.; Beavis, R. C.; Chait, B. T. Matrix-Assisted Laser Desorption Ionization Mass-Spectrometry of Biopolymers. *Anal. Chem.* **1991,** *63,* A1193–A1202.
14. Reinhold, V. N.; Reinhold, B. B.; Costello, C. E. Carbohydrate Molecular-Weight Profiling Sequence, Linkage, and Branching Data—ES, MS and CID. *Anal. Chem.* **1995,** *67,* 1772–1784.
15. Stahl, B.; Steup, M.; Karas, M.; Hillenkamp, F. Analysis of Neutral Oligosaccharides by Matrix-Assisted Laser Desorption-Ionization Mass-Spectrometry. *Anal. Chem.* **1991,** *63,* 1463–1466.
16. Whittal, R. M.; Palcic, M. M.; Hindsgaul, O.; Li, L. Direct Analysis of Enzymatic-Reactions of Oligosaccharide in Human Serum Using Matrix-Assisted Laser-Desorption Ionization Mass-Spectrometry. *Anal. Chem.* **1995,** *67,* 3509–3514.
17. Zaia, J. Mass Spectrometry of Oligosaccharides. *Mass Spectrom. Rev.* **2004,** *23,* 161–227.
18. Marshall, A. G. Milestones in Fourier Transform Ion Cyclotron Resonance Mass Spectrometry Technique Development; [Review]. *Int. J. Mass Spectrom.* **2000,** *200,* 331–356.
19. Hakansson, K.; Emmett, M. R.; Marshall, A. G.; Davidson, P.; Nilsson, C. L. Structural Analysis of 2D-Gel-Separated Glycoproteins from Human Cerebrospinal Fluid by Tandem High-Resolution Mass Spectrometry. *J. Proteome Res.* **2003,** *2,* 581–588.
20. Horn, D. M.; Zubarev, R. A.; McLafferty, F. W. Automated de Novo Sequencing of Proteins by Tandem High-Resolution Mass Spectrometry. *Proc. Natl. Acad. Sci. U.S.A.* **2000,** *97,* 10313–10317.
21. Pittman, J. L.; O'Connor, P. B. A Minimum Thickness Gate Valve with Integrated Ion Optics for Mass Spectrometry. *J. Am. Soc. Mass Spectrom.* **2005,** *16,* 441–445.
22. Jebanathirajah, J. A.; Pittman, J. L.; Thomson, B. A.; Budnik, B. A.; Kaur, P.; Rape, M.; Kirschner, M.; Costello, C. E.; O'Connor, P. B. Characterization of a New qQq-FTICR Mass Spectrometer for Post-Translational Modification Analysis and Top-Down Tandem Mass Spectrometry of Whole Proteins. J. Am. Mass Spectrom. **2005,** *16,* 1985–1999.
23. Gauthier, J. W.; Trautman, T. R.; Jacobson, D. B. Sustained Off-Resonance Irradiation for Collision-Activated Dissociation Involving Fourier-Transform Mass-Spectrometry—Collision-Activated Dissociation Technique That Emulates Infrared Multiphoton Dissociation. Anal. Chim. Acta **1991,** *246,* 211–225.
24. Mirgorodskaya, E.; O'Connor, P. B.; Costello, C. E. A General Method for Precalculation of Parameters for Sustained Off Resonance Irradiation/Collision-Induced Dissociation. *J. Am. Soc. Mass Spectrom.* **2002,** *13,* 318–324.
25. Little, D. P.; Speir, J. P.; Senko, M. W.; Oconnor, P. B.; McLafferty, F. W. Infrared Multiphoton Dissociation of Large Multiply-Charged Ions for Biomolecule Sequencing. *Anal. Chem.* **1994,** *66,* 2809–2815.
26. Zubarev, R. A.; Kelleher, N. L.; McLafferty, F. W. Electron Capture Dissociation of Multiply Charged Protein Cations. A Nonergodic Process. *J. Am. Chem. Soc.* **1998,** *120,* 3265–3266.
27. Zubarev, R. A.; Kruger, N. A.; Fridriksson, E. K.; Lewis, M. A.; Horn, D. M.; Carpenter, B. K.; McLafferty, F. W. Electron Capture Dissociation of Gaseous Multiply charged Proteins is Favored at Disulfide Bonds and Other Sites of High Hydrogen Atom Affinity. *J. Am. Chem. Soc.* **1999,** *121,* 2857–2862.
28. Leymarie, N.; Costello, C. E.; O'Connor, P. B. Electron Capture Dissociation Initiates a Free Radical Reaction Cascade. *J. Am. Chem. Soc.* **2003,** *125,* 8949–8958.
29. Adamson, J. T.; Hakansson, K. Electron Capture Dissociation of Oligosaccharides Ionized with Alkali, Alkaline Earth, and Transition Metals. *Anal. Chem.* **2007,** *79,* 2901–2910.
30. Budnik, B. A.; Haselmann, K. F.; Zubarev, R. A. Electron Detachment Dissociation of Peptide Dianions: An Electron-Hole Recombination Phenomenon. *Chem. Phys. Lett.* **2001,** *342,* 299–302.
31. Wolff, J. J.; Amster, I. J.; Chi, L.; Linhardt, R. J. Electron Detachment Dissociation of Glycosaminoglycan Tetrasaccharides. *J. Am. Soc. Mass Spectrom.* **2007,** *18,* 234–244.
32. Wolff, J. J.; Chi, L.; Linhardt, R. J.; Amster, I. J. Distinguishing Glucuronic from Iduronic Acid in Glycosaminoglycan Tetrasaccharides by Using Electron Detachment Dissociation. *Anal. Chem.* **2007,** *79,* 2015–2022.
33. Hakansson, K.; Cooper, H. J.; Emmett, M. R.; Costello, C. E.; Marshall, A. G.; Nilsson, C. L. Electron Capture Dissociation and Infrared Multiphoton Dissociation MS/MS of an N-Glycosylated Tryptic Peptide to Yield Complementary Sequence Information. *Anal. Chem.* **2001,** *73,* 4530–4536.
34. Hakansson, K.; Chalmers, M. J.; Quinn, J. P.; McFarland, M. A.; Hendrickson, C. L.; Marshall, A. G. Combined Electron Capture and Infrared Multiphoton Dissociation for Multistage MS/MS in a Fourier Transform Ion Cyclotron Resonance Mass Spectrometer. *Anal. Chem.* **2003,** *75,* 3256–3262.
35. Nielsen, M. L.; Savitski, M. M.; Zubarev, R. A. Improving Protein Identification Using Complementary Fragmentation Techniques in Fourier Transform Mass Spectrometry. *Mol. Cell. Proteom.* **2005,** *4,* 835–845.
36. McLafferty, F. W.; Fridriksson, E. K.; Horn, D. M.; Lewis, M. A.; Zubarev, R. A. Biochemistry-Biomolecule Mass Spectrometry. *Science* **1999,** *284,* 1289–1290.
37. Adamson, J. T.; Hakansson, K. Infrared Multiphoton Dissociation and Electron Capture Dissociation of High-Mannose Type Glycopeptides. *J. Proteome Res.* **2006,** *5,* 493–501.
38. Woodlin, R. L.; Bomse, D. S.; Beauchamp, J. L. Multiphoton Dissociation of Molecules with Low Power Continuous Wave Infrared Laser Radiation. *J. Am. Chem. Soc.* **1978,** *100,* 3248–3250.
39. Hakansson, K.; Cooper, H. J.; Hudgins, R. R.; Nilsson, C. L. High Resolution Tandem Mass Spectrometry for Structural Biochemistry. *Curr. Org. Chem.* **2003,** *7,* 1503–1525.
40. Huddleston, M. J.; Bean, M. F.; Carr, S. A. Collisional Fragmentation of Glycopeptides by Electrospray Ionization LCMS and LCMS-MS Methods for Selective Detection of Glycopeptides in Protein Digests. *Anal. Chem.* **1993,** *65,* 877–884.
41. Wilm, M.; Neubauer, G.; Mann, M. Parent Ion Scans of Unseparated Peptide Mixtures. *Anal. Chem.* **1996,** *68,* 527–533.
42. Kuster, B.; Krogh, T. N.; Mortz, E.; Harvey, D. J. Glycosylation Analysis of Gel-Separated Proteins. *Proteomics* **2001,** *1,* 350–361.
43. Mirgorodskaya, E.; Roepstorff, P.; Zubarev, R. A. Localization of O-Glycosylation Sites in Peptides by Electron Capture Dissociation in a Fourier Transform Mass Spectrometer. *Anal. Chem.* **1999>,** *71,* 4431–4436.
44. Mormann, M.; Macek, B.; de Peredo, A. G.; Hofsteenge, J.; Peter-Katalinic, J. Structural Studies on Protein O-Fucosylation by Electron Capture Dissociation. *Int. J Mass Spectrom.* **2004,** *234,* 11–21.
45. Kjeldsen, F.; Haselmann, K. F.; Budnik, B. A.; Sorensen, E. S.; Zubarev, R. A. Complete Characterization of Post-translational Modification Sites in the Bovine Milk Protein PP3 by Tandem Mass Spectrometry with Electron Capture Dissociation as the Last Stage. *Anal. Chem.* **2003,** *75,* 2355–2361.

46. Renfrow, M. B.; Cooper, H. J.; Tomana, M.; Kulhavy, R.; Hiki, Y.; Toma, K.; Emmett, M. R.; Mestecky, J.; Marshall, A. G.; Novak, J. Determination of Aberrant O-Glycosylation in the IgA1 Hinge Region by Electron Capture Dissociation Fourier Transform-Ion Cyclotron Resonance Mass Spectrometry. *J. Biol. Chem.* **2005,** *280,* 19136–19145.
47. Patel, T.; Bruce, J.; Merry, A.; Bigge, C.; Wormald, M.; Jaques, A.; Parekh, R. Use of Hydrazine to Release in Intact and Unreduced Form Both N-Linked and O-Linked Oligosaccharides from Glycoproteins. *Biochemistry* **1993,** *32,* 679–693.
48. Wing, D. R.; Rademacher, T. W.; Field, M. C.; Dwek, R. A.; Schmitz, B.; Thor, G.; Schachner, M. Use of Large-Scale Hydrazinolysis in the Preparation of N-Linked Oligosaccharide Libraries: Application to Brain Tissue. *Glycoconj. J.* **1992,** *9,* 293–301.
49. Takasaki, S.; Mizuochi, T.; Kobata, A. Hydrazinolysis of Asparagine-Linked Sugar Chains to Produce Free Oligosaccharides. *Methods Enzymol.* **1982,** *83,* 263–268.
50. Tarentino, A. L.; Plummer, T. H. Enzymatic Deglycosylation of Asparagine-Linked Glycans: Purification, Properties, and Specificity of Oligosaccharide-Cleaving Enzymes from Flavobacterium Meningosepticum. *Methods Enzymol.* **1994,** *230,* 44–57.
51. Harvey, D. J.; Bateman, R. H.; Green, M. R. High-Energy Collision-Induced Fragmentation of Complex Oligosaccharides Ionized by Matrix-Assisted Laser Desorption/Ionization Mass Spectrometry. *J. Mass Spectrom.* **1997,** *32,* 167–187.
52. Domon, B.; Costello, C. E. A Systematic Nomenclature for Carbohydrate Fragmentations in FAB-MS MS Spectra of Glycoconjugates. *Glycoconj. J.* **1988,** *5,* 397–409.
53. Kovacik, V.; Hirsch, J.; Kovac, P.; Heerma, W.; Thomasoates, J.; Haverkamp, J. Oligosaccharide Characterization Using Collision-Induced Dissociation Fast-Atom-Bombardment Mass-Spectrometry—Evidence for Internal Monosaccharide Residue Loss. *J. Mass Spectrom.* **1995,** *30,* 949–958.
54. Brull, L. P.; Heerma, W.; Thomas-Oates, J.; Haverkamp, J.; Kovacik, V.; Kovac, P. Loss of Internal 1→6 Substituted Monosaccharide Residues from Underivatized and Per-O-Methylated Trisaccharides. *J. Am. Soc. Mass Spectrom.* **1997,** *8,* 43–49.
55. Warrack, B. M.; Hail, M. E.; Triolo, A.; Animati, F.; Seraglia, R.; Traldi, P. Observation of Internal Monosaccharide Losses in the Collisionally Activated Dissociation Mass Spectra of Anthracycline Aminodisaccharides. *J. Am. Soc. Mass Spectrom.* **1998,** *9,* 710–715.
56. Mattu, T. S.; Royle, L.; Langridge, J.; Wormald, M. R.; Wan den Steen, P. B.; Van Damme, J.; Opdenakker, G.; Harvey, D. J.; Dwek, R. A.; Rudd, P. M. O-Glycan Analysis of Natural Human Neutrophil Gelatinase B Using a Combination of Normal Phase-HPLC and Online Tandem Mass Spectrometry: Implications for the Domain Organization of the Enzyme. *Biochemistry* **2000,** *39,* 15695–15704.
57. Harvey, D. J.; Mattu, T. S.; Wormald, M. R.; Royle, L.; Dwek, R. A.; Rudd, P. M. "Internal residue Loss": Rearrangements Occurring During the Fragmentation of Carbohydrates Derivatized at the Reducing Terminus. *Anal. Chem.* **2002,** *74,* 734–740.
58. Lemoine, J.; Fournet, B.; Despeyroux, D.; Jennings, K. R.; Rosenberg, R.; Dehoffmann, E. Collision-Induced Dissociation of Alkali-Metal Cationized and Permethylated Oligosaccharides—Influence of the Collision Energy and of the Collision Gas for the Assignment of Linkage Position. *J. Am. Soc. Mass Spectrom.* **1993,** *4,* 197–203.
59. Gillece-Castro, B. L.; Burlingame, A. L. Oligosaccharide Characterization with High-Energy Collision-Induced Dissociation Mass Spectrometry. *Methods Enzymol.* **1990,** *193,* 689–712.
60. Harvey, D. J. Collision-Induced Fragmentation of Underivatized N-Linked Carbohydrates Ionized by Electrospray. *J. Mass Spectrom.* **2000,** *35,* 1178–1190.
61. Orlando, R.; Bush, C. A.; Fenselau, C. Structural-Analysis of Oligosaccharides by Tandem Mass-Spectrometry—Collisional Activation of Sodium Adduct Ions. *Biomed. Environ. Mass* **1990,** *19,* 747–754.
62. Adamson, J. T.; Håkansson, K. Electron Capture Dissociation of Oligosaccharides Ionized with Alkali, Alkaline Earth, and Transition Metals. *Anal. Chem.* **2007,** *79,* 2901–2910.
63. Park, Y. M.; Lebrilla, C. B. Application of Fourier Transform Ion Cyclotron Resonance Mass Spectrometry to Oligosaccharides. *Mass Spectrom. Rev.* **2005,** *24,* 232–264.
64. Xie, Y. M.; Lebrilla, C. B. Infrared Multiphoton Dissociation of Alkali Metal-Coordinated Oligosaccharides. *Anal. Chem.* **2003,** *75,* 1590–1598.
65. Feng, W. Y.; Gronert, C.; Fletcher, K. A.; Warres, A.; Lebrilla, C. B. The mechanism of C-Terminal Fragmentations in Alkali Metal Ion Complexes of Peptides. *Int. J. Mass Spectrom.* **2003,** *222,* 117–134.
66. Penn, S. G.; Cancilla, M. T.; Lebrilla, C. B. Fragmentation Behavior of Multiple-Metal-Coordinated Acidic Oligosaccharides Studied by Matrix-Assisted Laser Desorption Ionization Fourier Transform Mass Spectrometry. *Int. J. Mass Spectrom.* **2000,** *196,* 259–269.
67. Cancilla, M. T.; Penn, S. G.; Carroll, J. A.; Lebrilla, C. B. Coordination of Alkali Metals to Oligosaccharides Dictates Fragmentation Behavior in Matrix Assisted Laser Desorption Ionization Fourier Transform Mass Spectrometry. *J. Am Chem. Soc.* **1996,** *118,* 6736–6745.
68. Leavell, M. D.; Leary, J. A. Stabilization and Linkage Analysis of Metal-Ligated Sialic Acid Containing Oligosaccharides. *J. Am. Soc. Mass Spectrom.* **2001,** *12,* 528–536.
69. Leavell, M. D.; Leary, J. A. Dissociation Mechanisms for Metal N-Glycosides of N-Acetyl Neuraminic Acid. *Int. J. Mass Spectrom.* **2001,** *204,* 185–196.
70. Gaucher, S. P.; Leary, J. A. Influence of Metal Ion and Coordination Geometry on the Gas Phase Dissociation and Stereochemical Differentiation of N-Glycosides. *Int. J. Mass Spectrom.* **2000,** *197,* 139–148.
71. Smith, G.; Kaffashan, A.; Leary, J. A. Influence of Coordination Number and Ligand Size on the Dissociation Mechanisms of Transition Metal Monosaccharide Complexes. *Int. J. Mass Spectrom.* **1999,** *183,* 299–310.
72. Zheng, Y. J.; Ornstein, R. L.; Leary, J. A. A Density Functional Theory Investigation of Metal Ion Binding Sites in Monosaccharides. *J. Mol. Struct. Theochem.* **1997,** *389,* 233–240.
73. Budnik, B. A.; Haselmann, K. F.; Elkin, Y. N.; Gorbach, V. I.; Zubarev, R. A. Applications of Electron-Ion Dissociation Reactions for Analysis of Polycationic Chito-Oligosaccharides in Fourier Transform Mass Spectrometry. *Anal. Chem.* **2003,** *75,* 5994–6001.
74. Cody, R. B.; Freiser, B. S. Electron Impact Dissociation. *Int. J. Mass Spectrom. Ion Phys.* **1979,** *51,* 547–551.
75. Seymour, J. L.; Costello, C. E.; Zaia, J. The Influence of Sialylation on Glycan Negative Ion Dissociation and Energetics. *J. Am. Soc. Mass Spectrom.* **2006,** *17,* 844–854.
76. Pfenninger, A.; Karas, M.; Finke, B.; Stahl, B. Structural Analysis of Underivatized Neutral Human Milk Oligosaccharides in the Negative Ion Mode by Nano-Electrospray MSn. Part 1: Methodology. *J. Am. Soc. Mass Spectrom.* **2002,** *13,* 1331–1340.
77. Pfenninger, A.; Karas, M.; Finke, B.; Stahl, B. Structural Analysis of Underivatized Neutral Human Milk Oligosaccharides in the Negative Ion Mode by Nano-Electrospray MSn. Part 2: Application to isomeric mixtures. *J. Am. Soc. Mass Spectrom.* **2002,** *13,* 1341–1348.
78. Karas, M.; Bahr, U.; Dulcks, T. Nano-Electrospray Ionization Mass Spectrometry: Addressing Analytical Problems Beyond Routine. *Fresen J. Anal. Chem.* **2000,** *366,* 669–676.
79. Solouki, T.; Reinhold, B. B.; Costello, C. E.; O'Malley, M.; Guan, S. H.; Marshall, A. G. Electrospray Ionization and Matrix-Assisted Laser Desorption/Ionization Fourier Transform Ion Cyclotron Resonance Mass Spectrometry of Permethylated Oligosaccharides. *Anal. Chem.* **1998,** *70,* 857–864.
80. Chaplin, M. F.; Kennedy, J. F. *Carbohydrate Analysis: A Practical Approach*, 2nd ed.; Oxford University Press: Oxford, 1994.
81. Ciucanu, I.; Kerek, F. A Simple and Rapid Method for the Permethylation of Carbohydrates. *Carbohydr. Res.* **1984,** *131,* 209–217.
82. Ciucanu, I.; Costello, C. E. Elimination of Oxidative Degradation during the Per-O-Methylation of Carbohydrates. *J. Am. Chem. Soc.* **2003,** *125,* 16213–16219.
83. Loboda, A.; Krutchinsky, A.; Loboda, O.; McNabb, J.; Spicer, V.; Ens, W.; Standing, K. G. Novel LINAC II Electrode Geometry for Creating an Axial Field in a Multipole Ion Guide. *Eur. J. Mass Spectrom.* **2000,** *6,* 531–536.
84. Wilcox, B. E.; Hendrickson, C. L.; Marshall, A. G. Improved Ion Extraction from a Linear Octopole Ion Trap: SIMION Analysis and Experimental Demonstration. *J. Am. Mass Spectrom.* **2002,** *13,* 1304–1312.
85. Tsybin, Y. O.; Hakansson, P.; Budnik, B. A.; Haselmann, K. F.; Kjeldsen, F.; Gorshkov, M.; Zubarev, R. A. Improved Low-Energy Electron Injection Systems for High Rate Electron Capture Dissociation in Fourier Transform Ion Cyclotron Resonance Mass Spectrometry. *Rapid Commun. Mass Spectrom.* **2001,** *15,* 1849–1854.
86. Fu, D.; Chen, L.; O'Neill, R. A. A Detailed Structural Characterization of Ribonuclease B Oligosaccharides by 1H NMR Spectroscopy and Mass Spectrometry. *Carbohydr. Res.* **1994,** *261,* 173–186.
87. Horn, D. M.; Zubarev, R. A.; McLafferty, F. W. Automated de Novo Sequencing of Proteins by Tandem High-Resolution Mass Spectrometry. *Proc. Natl. Acad. Sci U.S.A.* **2000,** *97,* 10313–10317.
88. O'Connor, P. B.; Costello, C. E. A High Pressure Matrix-Assisted Laser Desorption/Ionization Fourier Transform Mass Spectrometry Ion Source for Thermal Stabilization of Labile Biomolecules. *Rapid Commun. Mass Spectrom.* **2001,** *15,* 1862–1868.
89. Harvey, D. J. Structural Determination of N-Linked Glycans by Matrix-Assisted Laser Desorption/Ionization and Electrospray Ionization Mass Spectrometry. *Proteomics* **2005,** *5,* 1774–1786.
90. O'Connor, P. B.; Mirgorodskaya, E.; Costello, C. E. High Pressure Matrix-Assisted Laser Desorption/Ionization Fourier Transform Mass Spectrometry for Minimization of Ganglioside Fragmentation. *J. Am. Soc. Mass Spectrom.* **2002,** *13,* 402–407.
91. Zhang, J. H.; LaMotte, L. T.; Dodds, E. D.; Lebrilla, C. B. Atmospheric Pressure MALDI Fourier Transform Mass Spectrometry of Labile Oligosaccharides. *Anal. Chem.* **2005,** *77,* 4429–4438.
92. Hudgins, R. R.; Hakansson, ; Quinn, J. P.; Hendrickson, C. L.; Marshall, A. G. Electron Capture Dissociation of Peptides and Proteins Does Not Require a Hydrogen Atom Mechanism. *Proceedings of the 50th Annual Conference on Mass Spectrometry and Allied Topics*; Dallas, Texas. June, 2002.
93. Iavarone, A. T.; Paech, K.; Williams, E. R. Effects of Charge State and Cationizing Agent on the Electron Capture Dissociation of a Peptide. *Anal. Chem.* **2004,** *76,* 2231–2238.
94. Horn, D. M.; Ge, Y.; McLafferty, F. W. Activated Ion Electron Capture Dissociation for Mass Spectral Sequencing of Larger (42 kDa) Proteins. *Anal. Chem.* **2000,** *72,* 4778–4784.